Influence of Copper(I) Halides on the Reactivity of Aliphatic Carbodiimides [†]

Valentina Ferraro * and Marco Bortoluzzi

Dipartimento di Scienze Molecolari e Nanosistemi, Università Ca' Foscari, Via Torino 155, 30170 Mestre (VE), Italy; markos@unive.it

* Correspondence: valentina.ferraro@unive.it; +39-041-234-8651

† Presented at the 24th International Electronic Conference on Synthetic Organic Chemistry, 15 November–15 December 2020; Available online: https://ecsoc-24.sciforum.net/.

Abstract: The influence of copper(I) halides CuX (X = Cl, Br, I) on the electronic structure of *N,N'*-diisopropylcarbodiimide (DICDI) and *N,N'*-dicyclohexylcarbodiimide (DCC) was investigated by means of computational DFT methods. The coordination of the considered carbodiimides occurs by one of the nitrogen atoms, with the formation of linear complexes having general formula [CuX(carbodiimide)]. Besides varying the carbon-nitrogen bond lengths, the thermodynamically favourable interaction with Cu(I) reduces the electron density on the carbodiimides and alters the energies of the [NCN]-centred unoccupied orbitals. A small dependence of these effects on the choice of the halide is observable. The computed Fukui functions suggest negligible interaction of Cu(I) with incoming nucleophiles, and the reactivity of carbodiimides is altered by coordination mainly because of the increased electrophilicity of the [NCN] fragments.

1. Introduction

Carbodiimides are heteroallenes that play a crucial role in synthetic organic chemistry and biochemistry. Selected examples of the most important reactions are oligomerizations and polymerizations, cycloadditions, insertions and interactions with nucleophiles. As an example, carbodiimides are used with dimethylsulfoxide for the mild oxidation of alcohols to ketones. Moreover, carbodiimides find application in several condensation reactions, and the most noticeable example is the formation of peptide bonds from carboxylic acids and amines. As dehydrating agents, carbodiimides are used in reactions such as the conversion of primary amides to nitriles and of β-hydroxy ketones to α,β-unsaturated ketones, and they are involved in the synthesis of β-lactam antibiotics and nucleotides [1–4].

The most widely exploited carbodiimides in organic synthesis are diisopropylcarbodiimide (DICDI) and dicyclohexylcarbodiimide (DCC). The electrophilicity of carbodiimides can be enhanced by the addition of copper(I) halides to the reaction medium. For instance, the reaction of β-hydroxy ketones with DCC/CuCl affords α,β-unsaturated ketones, while α-cyclopropyl ketones can be obtained using γ-hydroxy ketones as reactants [5,6]. DCC/CuCl reacts with 2-hydroxyimines and nitroaldols to afford 2,3-enimines and nitroalkenes [7,8]. Isoureas, useful alkylating agents also involved in the preparation of heterocyclic compounds, are commonly obtained from the reaction of carbodiimides with alcohols in the presence of catalytic CuX [9–15]. The mild reaction conditions typical of Cu(I) catalysis provide an alternative and selective synthetic approach with respect to the utilization of Brønsted acids, that can promote oligomerization or interfere with other functional groups. For example, aliphatic carbodiimides undergo rapid dimerization catalyzed by

tetrafluoroboric acid at room temperature to give salts of the cyclodimers 1,3-dialkyl-2,4-bisalkylimino-1,3-diazetidines [16].

The catalytic action of copper halides apparently consists in the formation of coordination complexes with carbodiimides, but scarce experimental evidences are provided in the literature. In this work the interaction of DICDI and DCC with CuX (X = Cl, Br, I) is investigated by means of DFT calculations, and the influence of coordination on the electronic structure of carbodiimides is studied by several population analyses.

2. Methods

The computational geometry optimizations of DICDI, DCC and of the corresponding CuX complexes were carried out without symmetry constrains, using the range-separated hybrid functional ωB97X [17–19] and the def2 split-valence polarized basis set of Ahlrichs and Weigend, with relativistic ECP for iodine (28 electrons included in the pseudopotential) [20,21]. The "restricted" approach was applied for the free carbodiimides and the neutral copper complexes, while "unrestricted" single point calculations were carried out for the corresponding mono-anionic species. The electron densities were used for the plot of $f_+(r)$ Fukui functions [22]. The C-PCM implicit solvation model was added to ωB97X calculations, considering dichloromethane as continuous medium (dielectric constant = 8.93, refractive index = 1.424) [23,24]. The software used was ORCA 4.2.0 [25,26].

The output, converted in.molden format, was used for Mulliken and Hirshfeld charge distributions [27,28], Mayer and Wiberg bond order analysis [29,30] AIM analysis [31], electrostatic potential calculations, charge decomposition analysis (CDA) and extended charge decomposition analysis (ECDA) [32,33]. The software used was Multiwfn, version 3.5 [34]. All the calculations were performed with Intel Xeon-based x84-64 workstations.

3. Results and Discussion

The optimized geometries of DICDI, DCC and of the Cu(I) complexes [CuX(DICDI)] and [CuX(DCC)] are superimposed in Figure 1. All the attempts afforded as stationary points linear complexes with the carbodiimide κ^1-coordinated to Cu(I) by a nitrogen atom, ruling out the possibility of η^2-coordination by the C=N bonds.

Selected bond lengths are compared in Table 1. As observable, the coordination affects the carbon-nitrogen bond lengths, with the C=N and C-N bonds involving the coordinating nitrogen atom that become slightly longer, while the other C=N bond is shorter in the coordination compounds with respect to the free carbodiimides. These variations, comparable between DICDI and DCC, do not depend upon the nature of X. The N=C=N angle is not influenced by coordination, and it falls in the 174–175° range for all the considered species. The N-Cu distances are similar among all the complexes, in the 1.929–1.938 Å range, the slightly longer values corresponding to the heavier halide complexes. Accordingly, the Gibbs energy variations for the reactions carbodiimide + CuX→[CuX(carbodiimide)] are more negative for X = Cl (average ΔG = −39.5 kcal mol⁻¹) with respect to X = Br (average ΔG = −38.5 kcal mol⁻¹) and X = I (average ΔG = −36.8 kcal mol⁻¹). Such a trend can be explained on the basis of the softness of Cu(I) as metal centre and of the increasing softness of the halides along their group.

The variations in the carbon-nitrogen bonds are well highlighted by the Mayer and Wiberg bond orders, reported in Table 2. The C1-N3 interaction loses part of its double bond nature, and also the weakening of the N3-C5 bond is confirmed. According to the computed bond lengths, the C1-N2 bond is enforced by the coordination of the carbodiimides to CuX. Further confirmation comes from the density (ρ) and potential energy density (V) values at carbon-nitrogen (3,-1) bond critical points (b.c.p.), reported in Table 3. The ρ values for the C1-N3 and N3-C5 b.c.p. decrease (and the corresponding V values become less negative) moving from free to coordinated carbodiimides, while the opposite behaviour is shown by the C1-N2 b.c.p.
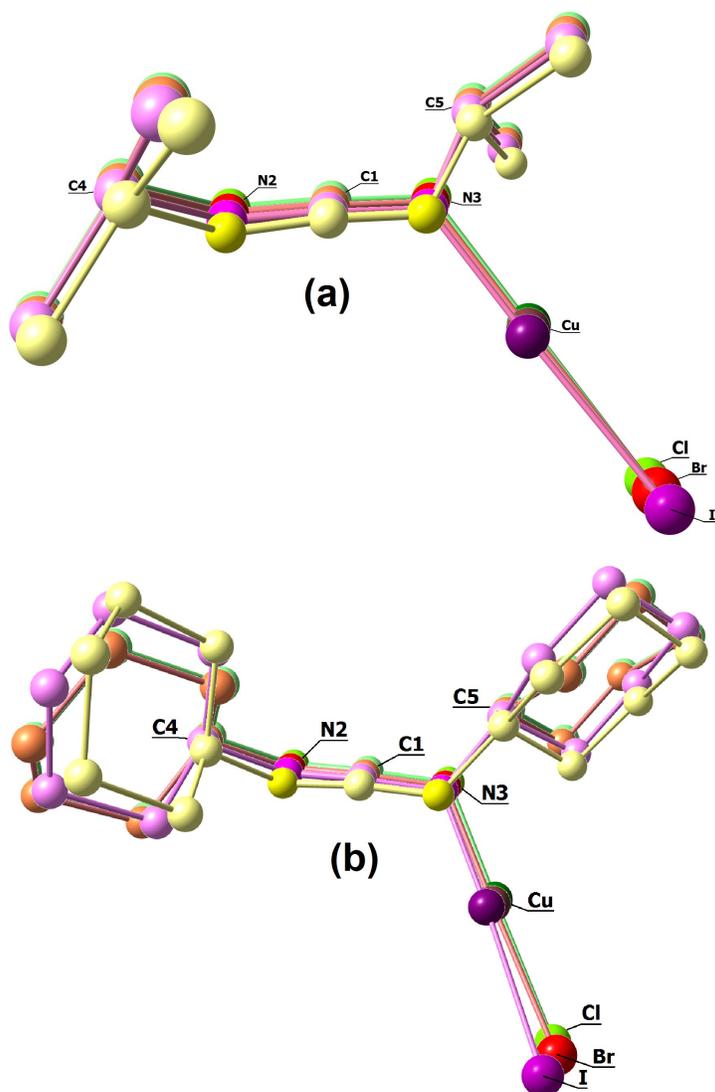
Figure 1. DFT-optimized structures of: (**a**) DICDI and [CuX(DICDI)]; (**b**) DCC and [CuX(DCC)]. Free carbodiimides, yellow tones; CuCl complexes, green tones; CuBr complexes, red tones; CuI complexes, violet tones. Hydrogen atoms are omitted for clarity. Selected captions were added for clarity.

Table 1. Selected computed bond lengths (Å) for carbodiimides and CuX complexes.

Bond	DICDI	[CuCl(DICDI)]	[CuBr(DICDI)]	[CuI(DICDI)]
C1-N2	1.217	1.193	1.193	1.193
C1-N3	1.215	1.243	1.243	1.243
N2-C4	1.478	1.470	1.470	1.470
N3-C5	1.471	1.494	1.494	1.494
Bond	**DCC**	**[CuCl(DCC)]**	**[CuBr(DCC)]**	**[CuI(DCC)]**
C1-N2	1.216	1.192	1.192	1.191
C1-N3	1.217	1.243	1.244	1.244
N2-C4	1.469	1.465	1.464	1.464
N3-C5	1.470	1.489	1.489	1.488

Table 2. Selected computed Mayer bond orders (Wiberg bond orders in parenthesis).

Bond	DICDI	[CuCl(DICDI)]	[CuBr(DICDI)]	[CuI(DICDI)]
C1-N2	2.107	2.217	2.217	2.216
	(2.393)	(2.490)	(2.490)	(2.491)
C1-N3	2.112	1.692	1.693	1.683
	(2.377)	(2.085)	(2.086)	(2.088)
N2-C4	0.864	0.842	0.842	0.842
	(1.196)	(1.164)	(1.164)	(1.165)
N3-C5	0.804	0.711	0.710	0.714
	(1.179)	(1.096)	(1.097)	(1.098)
Bond	**DCC**	**[CuCl(DCC)]**	**[CuBr(DCC)]**	**[CuI(DCC)]**
C1-N2	2.072	2.196	2.198	2.199
	(2.386)	(2.487)	(2.489)	(2.493)
C1-N3	2.083	1.700	1.700	1.682
	(2.379)	(2.078)	(2.078)	(2.077)
N2-C4	0.859	0.867	0.868	0.842
	(1.200)	(1.171)	(1.171)	(1.172)
N3-C5	0.837	0.629	0.627	0.664
	(1.181)	(1.102)	(1.102)	(1.104)

Table 3. Energy density (ρ) values at carbon-nitrogen (3,-1) bond critical points (b.c.p.). Potential energy density (V) values in parenthesis. Data in a.u.

Bond	DICDI	[CuCl(DICDI)]	[CuBr(DICDI)]	[CuI(DICDI)]
C1-N2	0.436	0.450	0.450	0.450
	(−1.340)	(−1.506)	(−1.505)	(−1.505)
C1-N3	0.435	0.418	0.419	0.419
	(−1.325)	(−1.159)	(−1.161)	(−1.161)
N2-C4	0.248	0.241	0.241	0.241
	(−0.410)	(−0.443)	(−0.442)	(−0.443)
N3-C5	0.248	0.236	0.236	0.236
	(−0.404)	(−0.374)	(−0.374)	(−0.375)
Bond	**DCC**	**[CuCl(DCC)]**	**[CuBr(DCC)]**	**[CuI(DCC)]**
C1-N2	0.435	0.449	0.450	0.451
	(−1.330)	(−1.507)	(−1.509)	(−1.513)
C1-N3	0.435	0.418	0.418	0.419
	(−1.327)	(−1.153)	(−1.152)	(−1.142)
N2-C4	0.249	0.243	0.243	0.243
	(−0.414)	(−0.459)	(−0.461)	(−0.463)
N3-C5	0.248	0.239	0.239	0.239
	(−0.412)	(−0.385)	(−0.385)	(−0.385)

Primary assessment of the influence of CuX coordination on DICDI and DCC is given by charge decomposition analyses (CDA and ECDA). Net donation of electron density from carbodiimide to CuX, in the 0.237–0.255 a.u. range, is obtained from CDA calculations. This result is confirmed by the ECDA analysis, with computed carbodiimide→CuX donations between 0.374 and 0.415 a.u. Despite the slight reduction of thermodynamic stability of the complexes, an increased electron density transfer is achieved by considering the heavier halides (see Table 4).

The role of coordination is clearly detectable by investigating the molecular orbitals of free and coordinated carbodiimides. In particular, the frontier unoccupied molecular orbitals of DICDI and DCC are mainly localized on the [NCN] fragments, and the bond with CuX introduces σ^*-type interactions with d-type orbitals of Cu(I). The orbital energies are meaningfully lowered, and the LUMO+1 orbitals in free carbodiimides correspond to the LUMO orbitals in [CuX(carbodiimide)] complexes, with an average energy reduction around 1.5 eV, as depicted in Figure 2 for DICDI and its derivatives. The energy lowering is more accentuated for the heavier halides, accordingly to the greater carbodiimide→CuX electron density donation reported in Table 4. The lower energy of

[NCN]-centred unoccupied orbitals reasonably makes more efficient the overlap with frontier occupied orbitals of electron-rich reactants. The σ^*(Cu-N) nature of LUMO and LUMO+1 in [CuX(carbodiimide)] could favour the Cu-N bond break after the nucleophilic attack, thus helping the catalytic activity of Cu(I) halides.

In spite of the different molecular orbital structure, the comparison of Fukui $f_+(r)$ functions between free and coordinates carbodiimides does not indicate important variations of the molecular regions involved in the interaction with nucleophiles (see for instance the inset of Figure 2). In all the cases the [NCN] fragment is almost exclusively affected, while the interaction of Cu(I) with incoming nucleophiles is predicted to be negligible, despite the unsaturated coordination sphere of the metal centre. Accordingly, the [CuX(carbodiimide)] molecular orbital diagrams do not show any low energy unoccupied orbital with proper orientation to interact with electron-rich species. On the basis of these outcomes, it appears that Cu(I) halides essentially act as Lewis acids for the activation of aliphatic carbodiimides.

Table 4. CDA values for the [CuX(carbodiimide)] complexes. ECDA values in parenthesis. Data in a.u.

Carbodiimide	CuCl	CuBr	CuI
DICDI	0.237	0.248	0.255
	(0.374)	(0.391)	(0.415)
DCC	0.240	0.251	0.254
	(0.379)	(0.398)	(0.415)
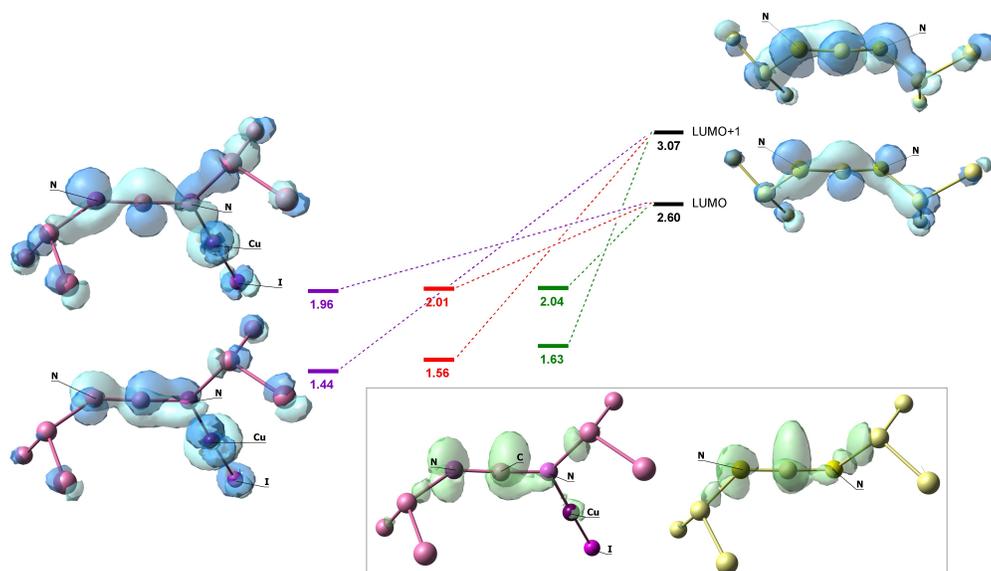
Figure 2. Energy values (eV) of LUMO and LUMO+1 orbitals of DICDI (black levels) and of its CuCl (green levels), CuBr (red levels) and CuI (violet levels) complexes. Plots of the LUMO and LUMO+1 molecular orbitals of DICDI (yellow tones) and of [CuI(DICDI)] (violet tones). Molecular orbitals surfaces in blue tones, isovalue = 0.05 a.u. Inset: plots of the Fukui $f_+(r)$ functions for DICDI and [CuI(DICDI)], surfaces in green, isovalue = 0.005 a.u. Hydrogen atoms are omitted for clarity.

The influence of coordination can be quantified by studying the partial charges variation of DICDI and DCC after coordination. The Hirshfeld population analyses show an increase of the C1 partial charge in the 0.045–0.047 a.u. range. The charge on the coordinating nitrogen atom (N3) is also more positive in the complexes with respect to the free carbodiimides by a comparable quantity (0.040–0.043 a.u.). Interestingly, the most important charge variation affects the non-coordinating nitrogen (N2), its Hirshfeld charge increasing by 0.074 a.u. in [CuX(DICDI)] complexes and by about 0.082 a.u. in [CuX(DCC)] derivatives. The meaningful increase of electrophilicity of C1 and N2 is

confirmed by the Mulliken population analyses, as observable from the data provided in Table 5. The partial charges can be explained from a Lewis structure point of view on considering that the donation to Cu(I) causes the partial delocalization of the N2 lone pair on the C1=N2 bond. Such a model is in agreement with the previously described enforcement of the C1=N2 bond caused by coordination. The increased electrophilicity of the [NCN] fragments is well highlighted also by the comparison of the electrostatic potentials of free and coordinated carbodiimides, as shown as example in Figure 3 for DICDI and its CuCl complex.

Table 5. Selected Hirshfeld partial charges. Mulliken charges in parenthesis. Data in a.u.

Atom	DICDI	[CuCl(DICDI)]	[CuBr(DICDI)]	[CuI(DICDI)]
C1	0.152	0.199	0.199	0.199
	(0.219)	(0.345)	(0.345)	(0.355)
N2	−0.184	−0.110	−0.110	−0.110
	(−0.346)	(−0.211)	(−0.211)	(−0.212)
N3	−0.184	−0.142	−0.141	−0.142
	(−0.339)	(−0.303)	(−0.289)	(−0.275)
C4	0.040	0.054	0.054	0.054
	(0.103)	(0.071)	(0.071)	(0.071)
C5	0.039	0.048	0.048	0.048
	(0.105)	(0.073)	(0.074)	(0.074)
Atom	**DCC**	**[CuCl(DCC)]**	**[CuBr(DCC)]**	**[CuI(DCC)]**
C1	0.154	0.199	0.200	0.199
	(0.210)	(0.327)	(0.326)	(0.325)
N2	−0.189	−0.108	−0.107	−0.107
	(−0.354)	(−0.206)	(−0.205)	(−0.205)
N3	−0.182	−0.142	−0.142	−0.144
	(−0.329)	(−0.325)	(−0.311)	(−0.287)
C4	0.032	0.046	0.046	0.046
	(0.118)	(0.041)	(0.041)	(0.069)
C5	0.034	0.041	0.040	0.040
	(0.074)	(0.110)	(0.112)	(0.098)
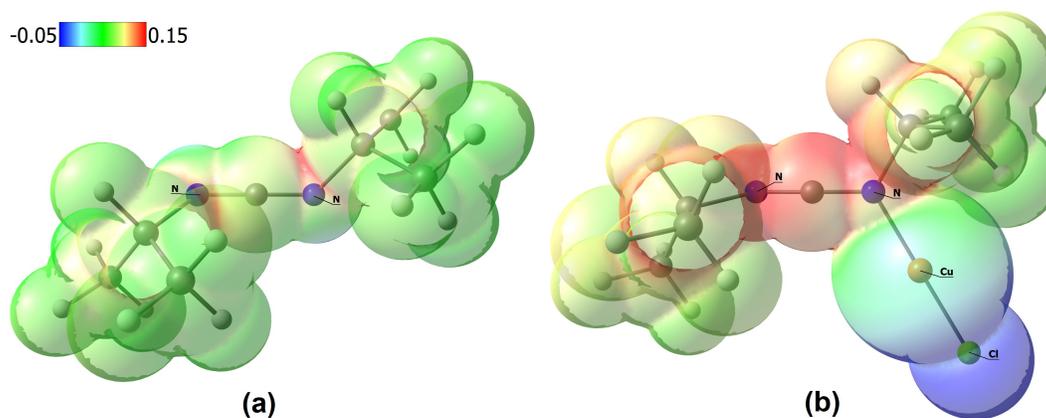
Figure 3. Overlapping spheres plots of DICDI (**a**) and [CuCl(DICDI)] (**b**) with mapped electrostatic potentials (a.u.).

4. Conclusions

DFT calculations confirm that aliphatic carbodiimides such as DICDI and DCC can coordinate Cu(I) halides with the formation of linear complexes, and that the interaction alters the orbital structure, the bond orders and the electrophilicity, enhancing the reactivity towards nucleophiles. The CuX fragments essentially behave as Lewis acids, and the nature of X influences to some extent aspects such as the Cu-N bond strength, the carbodiimide→CuX donation and the energies of

frontier unoccupied orbitals. Despite the fact that CuCl is actually the most employed catalyst in combination with carbodiimides, some of the results here provided suggest that the reactivity could be yet more enhanced by its replacement with CuI.

References

1. Khorana, H.G. The Chemistry of Carbodiimides. *Chem. Rev*. **1953**, *53*, 145−166, doi:10.1021/cr60165a001.
2. Kurzer, F.; Douraghi-Zadeh, K. Advances in the Chemistry of Carbodiimides. *Chem. Rev.* **1967**, *67*, 107−152, doi:10.1021/cr60246a001.
3. Williams, A.; Ibrahim, I.T. Carbodiimide chemistry: Recent advances. *Chem. Rev.* **1981**, *81*, 589−636, doi:10.1021/cr00046a004.
4. Ulrich, A. *Chemistry and Technology of Carbodiimides*; Wiley: Chichester, UK, 2007.
5. Schmidt, E.; Moosmüller, F. Zur Kenntnis aliphatischer Carbodiimide. *Liebigs Ann. Chem.* **1956**, *597*, 235−240, doi:10.1002/jlac.19555970307.
6. Alexandre, C.; Rouessac, F. La dicyclohexylcarbodiimide, agent de deshydratation intramoleculaire des cetols. *Tetrahedron Lett*. **1970**, *11*, 1011−1012, doi:10.1016/S0040-4039(01)97893-1.
7. Schuster, E.; Hesse, C.; Schumann, D. Dehydration of 2-Hydroxyimines with Dicyclohexylcarbodiimide: An Access to Cyclic Alkenylimines. *Synlett* **1991**, 916−918, doi:10.1055/s-1991-20922.
8. Knochel, P.; Seebach, D. Dehydratisierung von Nitroaldolen mit Dicyclohexylcarbodiimid: Herstellung von Nitroolefinen unter milden Bedingungen. *Synthesis* **1982**, 1017−1018, doi:10.1055/s-1982-30045.
9. Mathias, L.J. Esterification and Alkylation Reactions Employing Isoureas. *Synthesis* **1979**, 561−576, doi:10.1055/s-1979-28761.
10. Gibson, F.S.; Sook Park, M.; Rapoport, H. Bis[[4-(2,2-dimethyl-1,3-dioxolyl)]methyl]- carbodiimide (BDDC) and Its Application to Residue-Free Esterifications, Peptide Couplings, and Dehydrations. *J. Org. Chem*. **1994**, *59*, 7503−7507, doi:10.1021/jo00103a054.
11. Sinha, S.; Ilankumaran, P.; Chandrasekaran, S. One pot conversion of alcohols to disulfides mediated by benzyltriethylammonium tetrathiomolybdate. *Tetrahedron* **1999**, *55*, 14769−14776, doi:10.1016/S0040-4020(99)00939-4.
12. Schur, C.; Becker, N.; Bergsträßer, U.; Hartung, J.; Gottwald, T. Tertiary alkoxyl radicals from 3-alkoxythiazole-2(3H)-thiones. *Tetrahedron* **2011**, *67*, 2338−2347, doi:10.1016/j.tet.2010.12.071.
13. Kiełbasiński, P.; Żurawiński, R.; Orabowicz, J.; Mikołajczyk, M. Organosulphur compounds: XLVII Alkylation of sulphinic acids by o-alkylisoureas: O-versus s-reactivity and asymmetric synthesis of alkyl sulphinates. *Tetrahedron* **1988**, *44*, 6687−6692, doi:10.1016/S0040-4020(01)90108-5.
14. Bakibaev, A.A.; Shtrykova, V.V. Isoureas: Synthesis, properties, and applications. *Russ. Chem. Rev.* **1995**, *64*, 929−938, doi:10.1070/RC1995v064n10ABEH000185.
15. Bortoluzzi, M.; Paolucci, G.; Sartor, F.; Bertolasi, V. Synthesis and characterization of novel pyridine−isourea complexes of Pd(II). *Polyhedron* **2012**, *37*, 66−67, doi:10.1016/j.poly.2012.02.014.
16. Hartke, K.; Rossbach, F. Dimerisierung von Carbodiimiden. *Angew. Chem.* **1968**, *80*, 83, doi:10.1002/ange.19680800209.
17. Minenkov, Y.; Singstad, Å.; Occhipinti, G.; Jensen, V.R. The accuracy of DFT-optimized geometries of functional transition metal compounds: A validation study of catalysts for olefin metathesis and other reactions in the homogeneous phase. *Dalton Trans*. **2012**, *41*, 5526–5541, doi:10.1039/c2dt12232d.
18. Chai, J.-D.; Head-Gordon, M. Long-range corrected hybrid density functionals with damped atom–atom dispersion corrections. *Phys. Chem. Chem. Phys.* **2008**, *10*, 6615–6620, doi:10.1039/b810189b.
19. Gerber, I.C.; J. G.; Ángyán, J.G. Hybrid functional with separated range. *Chem. Phys. Lett.* **2005**, *415*, 100–105, doi:10.1016/j.cplett.2005.08.060.
20. Weigend, F.; Ahlrichs, R. Balanced basis sets of split valence, triple zeta valence and quadruple zeta valence quality for H to Rn: Design and assessment of accuracy. *Phys. Chem. Chem. Phys.* **2005**, *7*, 3297−3305, doi:10.1039/b508541a.

21. Peterson, K.A.; Figgen, D.; Goll, E.; Stoll, H.; Dolg, M. Systematically convergent basis sets with relativistic pseudopotentials. II. Small-core pseudopotentials and correlation consistent basis sets for the post-d group 16–18 elements. *J. Chem. Phys.* **2003**, *119*, 11113−11123, doi:10.1063/1.1622924.

22. Li, Y.; Evans, J.N.S. The Fukui Function: A Key Concept Linking Frontier Molecular Orbital Theory and the Hard-Soft-Acid-Base Principle. *J. Am. Chem. Soc.* **1995**, *117*, 7756−7759, doi:10.1021/ja00134a021.

23. Cossi, M.; Rega, N.; Scalmani, G.; Barone, V. Energies, structures, and electronic properties of molecules in solution with the C-PCM solvation model. *J. Comput. Chem.* **2003**, *24*, 669–681, doi:10.1002/jcc.10189.

24. Barone, V.; Cossi, M. Quantum Calculation of Molecular Energies and Energy Gradients in Solution by a Conductor Solvent Model. *J. Phys. Chem. A* **1998**, *102*, 1995–2001, doi:10.1021/jp9716997.

25. Neese, F. The ORCA program system. *WIREs Comput. Mol. Sci.* **2012**, *2*, 73–78, doi:10.1002/wcms.81.

26. Neese, F. Software update: The ORCA program system, version 4.0. *WIREs Comput. Mol. Sci.* **2018**, *8*, e1327, doi:10.1002/wcms.1327.

27. Cramer, C.J. *Essentials of Computational Chemistry*, 2nd ed.; Wiley: Chichester, UK, 2004.

28. Hirshfeld, R.F. Bonded-atom fragments for describing molecular charge densities. *Theor. Chim. Acta* **1977**, *44*, 129–138, doi:10.1007/BF00549096.

29. Mayer, I. Charge, bond order and valence in the AB initio SCF theory. *Chem. Phys. Lett.* **1983**, *97*, 270–274, doi:10.1016/0009-2614(83)80005-0.

30. Sizova, O.V.; Skripnikov, L.V.; Sokolov, A.Y. Symmetry decomposition of quantum chemical bond orders. *J. Mol. Struct. (THEOCHEM)* **2008**, *870*, 1–9, doi:10.1016/j.theochem.2008.08.021.

31. Bader, R.F.W. A quantum theory of molecular structure and its applications. *Chem. Rev.* **1991**, *91*, 893–928, doi:10.1021/cr00005a013.

32. Dapprich, S.; Frenking, G. Investigation of Donor-Acceptor Interactions: A Charge Decomposition Analysis Using Fragment Molecular Orbitals. *J. Phys. Chem.* **1995**, *99*, 9352–9362, doi:10.1021/j100023a009.

33. Gorelsky, S.I.; Ghosh, S.; Solomon, E.I. Mechanism of N_2O Reduction by the μ_4-S Tetranuclear Cu_Z Cluster of Nitrous Oxide Reductase. *J. Am. Chem. Soc*. **2006**, *128*, 278–290, doi:10.1021/ja055856o.

34. Lu, T.; Chen, F. Multiwfn: A multifunctional wavefunction analyzer. *J. Comput. Chem.* **2012**, *33*, 580−592, doi:10.1002/jcc.22885.